Microplastics in Surface Sediments of a Highly Urbanized Wetland

Farideh Amini Birami [a], Behnam Keshavarzi [a]*, Farid Moore [a], Rosa Busquets [b], Seyed Ghasem Ghorbanzadeh Zafarani [c], Reza Golshani [d], Hamidreza Cheshmvahm [a]

[a] Department of Earth Sciences, College of Science, Shiraz University, 71454 Shiraz, Iran

[b] School of Life Sciences, Pharmacy and Chemistry, Kingston University, Kingston Upon Thames, Surrey KT1 2EE, UK

[c] Research Center for Environment and Sustainable Development, RCESD, Department of Environment, Tehran, Islamic Republic of Iran

[d] Marine Environment and Wetlands, Department of the Environment, Iran

***Corresponding Author**

Tel-Fax: +98-71-32284572

Email:

bkeshavarzi@shirazu.ac.ir

Abstract

This study investigates the incidence of MPs in surface sediment samples, collected from the Anzali Wetland, Gillan province, North of Iran. This natural habitat receives municipal wastewater effluents and hosts industries and recreational activities that could release plastic to the wetland. There is need for studies to understand MPs pollution in wetlands. A total of 40 superficial sediment samples were taken covering potential pollution hotspots in the wetland. The average level of MPs was 362 ± 327.6 MPs/kg: the highest MPs levels were near the outlet of a highly urbanized river (Pirbazar River) (1380 MPs/kg), which runs through Rasht city. This was followed by 1255 MPs/kg where there was intense fishing, boating and tourism activities in the vicinity of Bandar-e Anzali city. Fibers were the most common type of MPs (80% of the total MPs detected). The MPs polluting the wetland were predominantly white/transparent (42%), and about 40% of them were >1000 μm. Polypropylene (PP) and polyethylene (PE) prevailed in MPs found. MPs were characterized with polarized light microscopy, Raman spectroscopy, Scanning Electron Microscopy coupled with Energy-Dispersive X-ray spectroscopy. Microplastics levels were found to correlate significantly ($p>0.7$) with electrical conductivity (EC) and sand-size fraction of the sediments. Coarse-grained sediments presented large capacity to lodge the MPs. This study can be used to establish protection policies in wetlands and newly highlights the opportunity of intercepting MPs in the Anzali Wetland, which are generally >250μm, before they fragment further.

Keywords: Microplastic; Anzali Wetland; Sediment; Wastewater

Highlights

- Microplastics were detected in all sampling sites in the Anzali Wetland (30 - 1380 MPs/kg).
- The highest MP concentrations were near urban areas and river mouths.
- Coarse-grained sediments have large capacity to lodge MPs load from wastewater.
- Large MPs (>1000 µm) are more prone to settle in the sediments of the wetland.

1. Introduction

Plastics are widely used and spread in the environment. It is difficult to calculate plastic release to the environment reliably (Qian et al., 2021). Approximately 6.3 billion tonnes of plastic had been generated until 2015 (Geyer et al., 2017). In a single year, 2010, ~ 4.8 - 12.7 million tonnes of plastic waste were transferred to the ocean, and there is an increasing trend with both plastic production and accumulation (Jambeck et al., 2015). Plastic pieces <5 mm are defined as microplastics (MPs) (Lambert et al., 2014). Microplastics are highly stable and can remain in the aquatic environment for a long time (Manbohi et al., 2021). The elimination of MPs from environmental matrices is not practicable yet (Bellasi et al., 2020). Therefore, MPs are now a global growing ecological concern (Dissanayake et al., 2022). MPs can be classed regarding their origin as primary and secondary MPs (Thompson, 2004). Primary MPs are made intentionally in the MPs size range, whereas secondary MPs originate gradually as a result of plastic degradation (Bellasi et al., 2020). Microplastics can act as vectors for several types of toxicants that can become adsorbed onto their surface owing to MPs' relatively high sorption capacities (Razeghi et al., 2021). Microplastics are potentially bioavailable and can be eaten erroneously as food by organisms (Wang et al., 2021). In the aquatic environments, 70% - 90% of the MPs deposit on surface and sub-surface sediment layers. Hence, sediments quality can be used in the assessment ecosystems' health (Yao et al., 2019). Wetlands provide ecological services for species and play a significant role in water filtration and stormwater management (Woodward and Wui, 2001). They are threatened by contaminants, and although important amounts of MPs end up in the marine environment via inland freshwater, there are insufficient studies on MPs pollution in wetlands sediments (Rasta et al., 2020; Yuan et al., 2019). Previous studies have reported that the discharge of wastewater effluents is a main source of MPs in wetlands (Naji et al., 2019; Rasta et al., 2020; Li et al., 2020; Edo et al., 2020; Helcoski et al., 2020) but they remain largely unexplored ecosystems regarding MP pollution.

The Anzali Wetland is a coastal wetland linked to the Caspian Sea located in the North of Iran. It was listed in the Montreux record as a site needing priority conservation, because it is confronted with high pollution load (Hassanzadeh et al., 2021). Due to the ecological and economic importance of the Anzali Wetland, several environmental studies have been conducted there (ALabdeh et al., 2020; Esmaeilzadeh et al., 2016a, 2016b; Hassanzadeh et al., 2021; Rasta et al., 2020; Shariati et al., 2019). Microplastics contaminating the wetlands were reported earlier in the sediment of the wetland (140-2820 and 113-3690 MPs/kg) (Rasta et al., 2020); in its surface water (0.40-4.41 and 0.19-2.85 MPs/m^3) (Rasta et al., 2020); and in fish tissues (1.1-2.26 MPs/individual) (Rasta et al., 2021) collected from a small area in the Anzali Wetland. Goals of this study are characterizing the levels and spatial distribution of MPs in superficial sediment samples from the Anzali Wetland and understanding the link between the MPs pollution in the wetland with its sources. This study will support the evaluation of the ecological risks of MPs in the wetland and will inform protection policies regarding plastic pollution for wetland areas in Iran.

2. Material and methods

2.1. Study area

The Anzali Wetland is located in the North of Iran (Gilan Province) and Southwest of the Caspian Sea (37°25′ to 37°30′N and 49°15′ to 49°30′E) (Fig. 1). The wetland (193 km^2) is rich in biota (Esmaeilzadeh et al., 2016b; Naderi and Saatsaz, 2020). The regional climate is predominantly subtropical and the average annual precipitation in this region is ~1200 mm (Naderi and Saatsaz, 2020). The catchment area of the wetland watershed is about 3610 km^2 (Amini et al., 2021), with approximately 969 K permanent residents, according to the 2017 census. The most populated cities in this catchment are Rash and Bandar-e Anzali cities with 680 K and 119 K inhabitants, respectively. Fig. 1 shows the study site, including the presence of semiconductor, electronic, and food industries. Additional information regarding the Anzali Wetland is given in Supporting Information S1.

2.2. Sample collection

A total of 40 superficial sediment samples were collected from the Anzali Wetland in June 2021 (Fig. 1). Samples were collected from the vicinity of Bandar-e Anzali city, which is affected by urbanization, boating traffic, tourist and fishing activities (A Group; A1 to A5); from outflow pathways that discharge the wetland's water into the Caspian Sea (B Group; B1 to B3); from the middle part of wetland (it may be impacted by shipping and fishing activities (C Group; C1 to C8)); from inflow pathways which may be contaminated by municipal, agricultural, and industrial wastewater of surrounding residential and agricultural areas (D Group; D1 to D24). Detailed information regarding sample preparation, extraction of MPs and analyses of physico-chemical parameters of the soil sediment samples can be found in Supporting Information (S2 to S5).

2.3. Identification of MPs

Physical characteristics of suspected MPs were recorded using a binocular stereoscopic microscope (ZTX-E up to × 80 magnification). The MPs were inspected optically considering the criteria proposed by Norén (2007) and Hidalgo-Ruz et al. (2012). Also, each particle that could potentially be made of plastic was verified as plastic with a hot needle. Based on birefringent properties of anisotropic MPs, polarized light microscopy (PLM) (PM, Olympus, Ramsey, NJ, USA) was used to verify our visual inspection (Lusher et al., 2013). The size of MPs was determined by measuring the longest dimension (L). They were divided into four classes (100 ≤L<250 μm, 250≤ L< 500 μm, 500≤ L< 1000 μm, and L≥1000 μm). Microplastics <100 μm were not counted due to possible visual error (Kershaw et al., 2019). The MPs were categorized by shape into three kinds (fiber, fragment and film) and by color into five categories (white/transparent, black/grey, red/pink, blue/green, and yellow/brown). The composition of a set of 40 randomly selected MPs was identified using an XploRA Plus confocal Raman spectroscopy (Jobin Yvon, HORIBA Gr, France) with IR-laser (785 nm, with maximum power = 100 mW). A 50%-filter controlled by software was used to decrease the laser power on samples. Raman shifted spectra was measured with 0.2 cm^{-1}/pixel spectral resolution in the range of 400 to 1800 cm^{-1} using an acquisition time of 15s. The device was calibrated by recording the Raman spectrum of pure silicon wafer as a sample reference. The HORIBA Scientific's Lab Spec 6 Software package was used for instrument control, spectra data collection, and analysis. Polymers were identified by matching spectra obtained by the one in the HORBIA Edition of the KnowltAll ® standard database. Surface morphological features of randomly selected MPs, along with the elemental composition of them, were analyzed by Scanning Electron Microscope (SEM, TESCAN Vega 3, Czech Republic) with a resolution of 2 nm at 20 kV armed with an energy-dispersive X-ray microanalyzer (EDS).

3. Results and discussion

3.1. Abundance and distribution of MPs

Microplastics were detected in all sediment samples (Fig. S1). A total of 2899 MPs were counted. Since MPs < 100 μm were not counted, there is some underestimation taking place. The obtained results were analyzed statistically (described in Supporting Information S6). The abundance of MPs varied from 6 to 276 MPs/200 g DW (dry weight) (i.e., 30 to 1380 MPs/kg sediment sample). The average value of MPs concentration was 362 ± 328 MPs/kg. Kolmogorov–Smirnov test indicated that MPs abundances were non-normally distributed ($p < 0.05$). The mean concentration of MPs in the group A (Fig. S1a), which are located in the vicinity of Bandar-e Anzali city, was higher than others. The average abundance of MPs among four sampling groups varied in the order A (659 ± 427 MPs/kg) > D (413 ± 312 MPs/kg) > B (163 ± 72 MPs/kg) >C (99 ± 67 MPs/kg) (Fig. S1a). A significant difference ($p = 0.001$) was observed between MPs abundance in different sampling groups.

The lowest levels of MPs were found in C5 (30 MPs/kg), C1 (35 MPs/kg), and C2 (45 MPs/kg) (Fig. S1b). These stations are located in the middle part of the wetland, suggesting that less impactful anthropogenic activities are taking place this part of the wetland (Fig. 1). The maximum abundances of MPs were in A5 (1255 MPs/kg) and D15 (1380 MPs/kg) (Fig. S1b). Those in A5 could be due to the presence of an extensive range of boating, tourism, recreational and fishing activities in the Bandar-e Anzali city that could release MPs to the wetland. In the study area, abundant rain can also intensify the transport of MPs from the watershed and urban areas into the Anzali Wetland via runoff and/or rivers (Zhou et al., 2020). A sediment sample from D15 was collected from the bed sediment of the Pirbazar River: the main source of water supplying the wetland. The Pirbazar River originates from the connection of two polluted rivers, Goharrood and Zarjoub. They pass-through Rasht city and enter the study wetland (Amini et al., 2021; Hassanzadeh et al., 2021). Previous research indicated that the Pirbazar River was one of the main entry routes of contamination from the catchment to the Anzali Wetland

(ALabdeh et al., 2020; Amini et al., 2021; Esmaeilzadeh et al., 2021). The Pirbazar River is a sink of untreated wastewater, urban runoffs, disposal waste, and landfill leachate. These findings evidence that it can transport substantial amounts of buoyant MPs, some of which settle in the sediment from the uplands toward the wetland. In contrast, farm equipment, atmospheric deposition, and plastic cases discarded from bird hunting were found less important sources of MPs in the Anzali Wetland (Rasta et al., 2020). The Anzali Wetland is a pathway that carries an important load of MPs pollution which may be brought to the Caspian Sea through several channels. Microplastic abundance in the B group of sampling stations (where samples were collected from outflow pathways) was lower than in the A and D groups. It could be that, in these sampling sites (A, D), the entrapped MPs in surficial sediments layers were washed away by water currents from the Caspian Sea. Furthermore, buoyant MPs in the B region cannot settle rapidly onto the wetland surface sediment due to the interaction between wetland water and seawater.

The average concentration of MPs in the sediment samples of the Anzali Wetland (362±327.6 MPs/kg) was higher than what was found in wetlands in the Persian Gulf (20 ± 6.36 to 35 ± 0.71 MPs/kg) (Naji et al., 2019) and Greater Melbourne (46 MPs/kg) (Townsend et al., 2019) (Table S1). These wetlands are situated in protected areas with a low level of human interference unlike the Anzali Wetland. In contrast, the sediments of the Yellow River Delta (136-2060 MPs/kg) (Duan et al., 2020); Queensland's Gold (595 ± 12 to 320 ± 42 MPs/kg) (Ziajahromi et al., 2020); Futian (2835 ± 713 MPs/kg) (Duan et al., 2021); East Kolkata (2125-6886.76 MPs/kg) (Sarkar et al., 2021); and Setiu Wetland (750 ± 3838 to 14250 ± 4343 MPs/kg) (Ibrahim et al., 2021), were affected by highly urbanized rivers, fisheries and aquaculture and also had relatively high MPs pollution. The mean abundance of MPs found in the present study was lower than in a previous study by Rasta et al. (2020) in the Anzali Wetland (784 ± 877.8 to 520 ± 1024.2 MPs/kg). The earlier study carried out sampling near the Bandar-e Anzali city: a hotspot of anthropogenic contaminants, whereas the present study involved a more general sampling in the entire Anzali Wetland.

3.2. Characterization of MPs

The collected MPs were classified into three major groups, namely fibers (Fig. 2a-c), fragments (Fig. 2d-f) and films (Fig. 2g-h). Although, some selected MPs showed clear birefringence properties under cross-polarized light (CPL) (Fig. 2i-l), it was not practical to verify all types of MPs by using this technique because most MPs did not show birefringent properties. Fibers were the most common shape of MPs (80%) followed by films (12%) and fragments (8%). Fibers were observed in all samples with a proportion of 37-100%, specifically the maximum numbers of fiber MPs were counted in A5 (1110 MPs/kg) and D15 (1285 MPs/kg) (Fig. 3a). This results agree with earlier research in the Anzali (Rasta et al., 2020), Yellow River Delta (Duan et al., 2020), Persian Gulf (Naji et al., 2019), Xijin (Wang et al., 2021), and Queensland's Gold (Ziajahromi et al., 2020) wetlands (Table S1). Microplastic fibers are released from garments. One garment can produce more than 1900 fibers per wash (Browne et al., 2011). This demonstrates that the dominant source of MPs in the study area could be domestic wastewater effluents input via local rivers and/or urban runoffs. Additionally, degradation of different types of worn or discarded commercial fishing gear like net and rope are potentially other sources of fibers in Anzali Wetland (Mehdinia et al., 2020). Naji et al. (2019) demonstrated that untreated effluent discharges from residential areas are the main source of fibers in sediments of the mangrove ecosystem in the northern coast of the Persian Gulf. Films can be originated from the fragmentation of discarded wrapping materials and plastic bags. These films can also break down further when transported over long distances in rivers (Soltani et al., 2022; Townsend et al., 2019). The maximum numbers of films were counted in A1 (160 MPs/kg), D4 (170 MPs/kg) and D17 (250 MPs/kg). The maximum number of fragments were counted in A1 (100 MPs/kg) and D18 (205 MPs/kg) (Fig. 3a).

The most abundant color of MPs were white/transparent and black/grey, with about 42% and 28% of the total, respectively (Fig. 3b, S2a). The high percentage of white/transparent MPs may be due to photobleaching and photodamage of their original colors by ultraviolet (UV) light (Firdaus et al., 2020). Yellow/brown, red/pink and blue/green were other identified colors in the samples (Fig. S2a), these MPs could have entered the environment recently. The variety of colors was higher than what was reported in a previous study (Rasta et al., 2020). Although, the original color of the MPs in sediment samples may be altered during weathering, biofilm formation, bleaching and erosion processes (Firdaus et al., 2020) as well as during sample preparation and MPs extraction processes (Soltani et al., 2022), it has been reported that wide variety of colors can be due to wide range of MPs sources (Mehdinia et al., 2020). Among the fiber MPs, white/transparent was their most common color (39%), followed by black/grey (28%) (Fig. S2b), which were also commonly recognized elsewhere (Table S1). The most prevalent color for fragments and films were black/grey (43%) and white/transparent (43%) (Fig. S2c and d). Also, the predominant color in A5 and D15 (the most contaminated stations) was white/transparent (Fig. 3b). This prevalent color points towards possible accumulation of plastic with time in these sites, which is revealed by the abundant fraction of plastics that could be white due to photobleaching.

Fig. 3c showed the percent distribution of size classes (in μm) of MPs in the study area. Microplastics sizes ranged approximately between 100 μm and 1500 μm with an average length of 950 μm. The prevalence lengths were in the range of $L \geq 1000$ μm (41%), followed by $500 \leq L < 1000$ μm (32%) (Fig. S3a). The predominant size of fiber, fragment, and film was $1000 \leq L$ μm (47%), $250 \leq L < 500$ μm (40%), and $500 \leq L < 1000$ μm (37%), respectively (Fig. S3b, c, and d). Approximately 91% of the MPs were >250 μm and 9% of them in the $100 \leq L < 250$ μm category (Fig. S3a).

Different MPs sources, MPs degradation degree, impact of weathering agents, composition of the polymer and laboratory procedures (e.g. sampling net cut-off, sample preparation steps including harsh chemical), and diagnostic errors can affect the size distribution of MPs reported in the study areas (Li et al., 2018). The results of the previous research in the wetland showed that fibers with 1000 to 2000 µm were the most abundant in Anzali Wetland (Rasta et al., 2020). Similarly, in the urban wetlands of Kenil worth Park (Li et al., 2020), Guangxi (Zhou et al., 2020), and Hainan (Zhou et al., 2020), fiber particles >1000 µm were dominant in sediments samples. This relatively big size can indicate that the fiber MPs are relatively "fresh" in the ecosystem and have not undergone further fragmentation caused by weathering.

The small MPs might remain floating in the water column, while the larger ones with densities slightly higher than water are more prone to settle at the bottom sediments of wetland (Nizzetto et al., 2016). The average size of fragments found in this study (~350 µm) was smaller than fibers (~ 900 µm) and films (~ 600 µm). The fragments have probably resulted from greater weathering of larger MPs or larger plastics than other types. The predominant relatively big fraction size of MPs (>250µm) is indicative that there is an opportunity to intercept these MPs before they fragment further into smaller MPs (<250 µm), which were found to prevail in other environmental compartments such as soil (Nematollahi et al., 2022).

3.3. Interrelations of MPs abundances

Principal component analysis (PCA) of the main five different colors of MPs found, main shape types and sizes classified in four ranges (the Kaiser–Meyer–Olkin values were higher than 0.7) are shown in Fig. 4a. Principal component 1 and 2 explained 68.75% and 11.60% of total variances contributing in both PCs. Fiber, film, white/transparent, yellow/brown, red/pink, blue/green, black/grey, $100 \leq L < 250$ µm, $500 \leq L < 1000$ µm, and $1000 \leq L$ µm fell in PC1 and had a strong correlation ($p > 0.5$) (Table S2 and S3), suggesting that they follow similar distribution in the sediment sampling stations. Fragment $250 \leq L < 500$ µm had greater influence in PC2 (Table S2), confirming that the majority of fragments are in that size range (Fig. S3c). Fragment have no significant positive relation with fiber and film, i.e., its eigenvectors make a very large angle (Table S2 and S3). This shows a different distribution of fragment in the samples and thus it likely originates from different sources and distribution routes. Fibers and films were prevalent in A and D sampling groups, whereas fragment were mainly associated with sites in A and B sampling groups. Sample scores in the PCA illustrated that A5 and D15 had a very strong positive score in PC1 (Fig. 4a), suggesting that these sampling sites greatly control the distribution of these types of MPs in the study area. Also, based on sample scores, MPs contamination in the Anzali Wetland was mainly released from A and D sampling groups.

The interrelations between MPs, the physico-chemical parameters and sampling groups are displayed in Fig. 4b. Principal component 1 and 2 explain 33.91% and 24.08% of total variances. The total concentration of MPs (fiber, fragment, and film), sand, and electrical conductivity (EC) fell in PC1 and this suggests that the occurrence of MPs in sediments can be impacted by these factors. Alternatively, silt, clay, pH, organic matter (OM), cation exchange capacity (CEC), and $CaCO_3$ had greater influence in PC2 (Table S4). There is no significant correlation between these parameters and MPs (Table S5). A strong positive relationship between MPs and EC ($p>0.7$) could be due to the input from domestic wastewater effluents via local rivers that may also receive urban runoffs. Suhogusoff et al. (2019) reported that wastewaters containing salts can contribute towards the total salt content and cause the increase of EC of the effluent.

Sediment grain size may influence MPs distribution. Studies have found that MPs are more abundant in fine grain sediments (Soltani et al., 2022; He et al., 2020; Liang et al., 2022). Nevertheless, there was no positive correlation between MPs and the clay fraction of samples in this study (Table S5). The high levels of MPs counted from fine-grained sediments are presumably the result of higher surface tension of fine particles (Soltani et al., 2022; Li et al., 2020). On the other hand, fine-grained sediments are known to be more cohesive (Nor and Obbard, 2014), which potentially hinders MPs filtration, unless sediments are in suspension. In this study, a strong positive relationship between MPs and sand ($p>0.9$) was found (Table S5).

It could be because coarse-grained sediments tend to have large interstitial pores, which could lodge MPs. This is supported by Govender et al. (2020) who found that MPs in sediment was positively correlated with coarse (500–2000 µm)-grained sediments.

3.4. Polymer composition

Typical Raman analysis spectra of some detected MPs are illustrated in Fig. S4. Polypropylene (PP; with a density of 0.92 g/cm^3), polycarbonates (PC; with a density of 1.2-1.22 g/cm^3), polyethylene terephthalate (PET; with a density of 1.38 g/cm^3), polyvinyl chloride (PVC; with a density of 1.38 g/cm^3), nylon (NYL; with a density of 1.15 g/cm^3), low-density polyethylene (LDPE; with a density of 0.910-0.925 g/cm^3), medium-density polyethylene (MDPE; with a density of 0.926–0.940 g/cm^3), and high-density polyethylene (HDPE; with a density of 0.93 to 0.97 g/cm^3) (Lusher, 2015) were detected from the selected MPs. The matching ratio between the experimental spectra and the database ranged between 75% and 90%. The match degrees can be affected by weathering, aging, and adherence of other substances (Li et al., 2018). The density of PC, PET, PVC, and NYL MPs was higher than that of seawater and freshwater, and hence they are expected to be immersed in the sediment after entering the wetland (Amaral-Zettler et al., 2021).

Deposition of light polymers (PP and PE) into the sediments may have been affected by biofouling, weathering, hetero-aggregation or biomolecule adsorption processes (Soltani et al., 2022). Also, adsorption and adhesion of foreign materials such as clay minerals or quartz grains in superficial pits, grooves and cracks of weathered MPs may alter sinking behavior of MPs (Zhou et al., 2018). In this study, adhered mineral substances were observed onto particles using SEM images (Fig. 5a, c, and d). Raman analysis indicated large variety of polymers within the fibers, which is presumably related to their numerous sources (Zhou et al., 2020). Our results were different from the previous study in Anzali Wetland. We did not detect polyester (PEST), polyacrylonitrile (PAN), and polystyrene (PS), which were reported by Rasta et al. (2020). It can be concluded that MPs with wide variety of polymeric compositions were deposited in the sediments of Anzali Wetland.

Polypropylene and PE were the main polymer types of MPs (35%), followed by NYL (13%). The types of polymer composition can link the MPs with their sources. Polypropylene and PE were the most reported polymers not only in the Anzali Wetland but also in other wetlands (Table S1). Since PP and PE are utilized to produce fishing nets and ropes, addition to untreated wastewaters, fishery and mariculture activities may be significant sources of these polymers (Chowdhury et al., 2017). Moreover, these polymers are frequently employed in manufacturing many products including clothes, supermarket bags, food containers, plastic bottles, bottle caps, and compact discs (Elvers, 2016). Nylon particles mainly may originate from clothes, ropes, fishing lines, and fishing nets, and PET fibers may release from textile (Wen et al., 2018). Polyvinyl chloride is applied in the manufacture of electric cables, bottles, pipes, and cups (Andrady, 2011). Polycarbonates is primary used in the production of disposable tableware, bottles, electronics, watch cases, the healthcare industry, medicine, safety goggles, home appliances, etc. (Maghsodian et al., 2021).

3.5. Morphology of MPs

In MPs studies, sample preparation, separation and imaging may change morphological characteristics of MPs (Soltani et al., 2022). Irregular fragments were found to be rough and eroded together with deformations, fractures, pits, flakes, and edged structures which signifies their weathering and mechanical fragmentations (Fig. 5a) (Ibrahim et al., 2021). Wang et al., (2017) concluded that the irregular shape of MPs indicates mechanical breakage. Films exhibited porous surfaces with common weathering and aging patterns such as cracks, pits, fractures, regular edge and grooves (Fig. 5b and c). The relatively uneven surfaces of most MPs demonstrate that they presumably have undergone several degrees of weathering processes. Fig. 5b showed two LDPE films with different degree of weathering. The spectra match of intensively weathered LDPE film (78%) was lower than that from moderately weathered LDPE film (85%). Fibers displayed a relatively linear and smooth surfaces (Fig. 5e and f), although signs of weak physical abrasion and chemical weathering as deformations and indentations are observed. The relatively soft morphology of the fibers suggests that most of them were derived from adjacent contamination sources, although due to weathering, some may degrade further into smaller MPs (Nematollahi et al., 2020).

3.6. Elemental composition of MPs

The EDX analysis indicated that C (47.7-85.1%) and O (10.7-28.2%) are major constituents of MPs (Fig. 5). Furthermore, trace amounts of some other elements including Na, Mg, Al, Si, Cl, K, Ca, Fe, Cu, Zn, and Ti were also identified. Since plastics are usually made of organic/inorganic substances and contain C, O, H, S, Si, and Cl (do Sul and Costa, 2014), other detected elements may be originated from chemical additives to polymers (do Sul and Costa, 2014), adsorption from external environments or chemicals used for MPs isolation (e.g. Zn, Cl) (Mehdinia et al., 2020). Titanium in the form of TiO_2 -NPs is added to polymer materials to make white pigments or UV blockers (Wang et al., 2017). Silica is commonly incorporated into thermoplastics in order to enhance plastic resistance. Iron is generally used as inorganic pigments to yield red and yellow colors (Nematollahi et al., 2021). Aluminum, Ca, Mg, Na, and Si are commonly used as additives to defer the oxidation of the plastic material. Moreover, geogenic Al, Ca, Si, and Mg can originate from natural materials such as soil or dust. Copper and Zn can be originated from burning fossil fuels and industrial activities, and they could be sorbed onto the MPs (Nematollahi et al., 2020).

There were differences in the relative amounts of C and O between fragment (C: 47.70% and O: 21.50%) (Fig. 5a) and fiber (C: 85.07% and O: 12.31%) (Fig. 6d) with same polymeric composition. The presence of a high level of O (W %) and low level of C (W %) in fragment can be a sign of intensive weathering (Soltani et al., 2022). Overall, the surfaces of fragments and films displayed signs of sever photochemical and mechanical weathering, but surfaces of fibers appeared to be largely intact. Weathering increases roughness of the surface of MPs and enhance their capability to adsorb various environmental contaminants (Mehdinia et al., 2020). Surface pits and grooves in MPs were filled with tiny irregular-shaped substances (Fig. 5a and b). As shown in Fig. 5, the percentage (W %) of detected trace elements in fragment and film were higher than in fiber.

4. Conclusion

This study demonstrates that superficial sediments of the Anzali Wetland were contaminated with MPs. Fiber-like particles, white/transparent, black/grey in color, L≥1000 μm in size, and PP and PE in polymer types dominated. Microplastic abundance showed a significant positive correlation with the sand fraction and EC. This points towards a potential role of coarse-grained sediments on the transport and ultimate fate of MPs load of wastewater in the Anzali Wetland. Furthermore, laboratory simulation experiments are recommended to examine these relationships. Untreated wastewaters inputs via local rivers and/or urban runoffs, as well as fishing, tourism, and recreational activities, probably were the essential parameters that should be monitored in the studies of MPs sources of the Anzali Wetland. From the new information found by this study, there is urgent need for domestic and industrial wastewater treatment systems and plastic waste regulation plans in areas affecting wetlands. Our results present the assessment of the status of MPs pollution in the Anzali Wetland and can be used to know the estate of the pollution, necessity to remediate the site and stop relevant emissions causing such pollution.

Acknowledgment

The authors sincerely appreciate the Research Committee and Medical Gology Center of Shiraz University for logistical assistance. Thanks are extended to the Research Center for

Environment and Sustainable Development (RCESD) of Iranian Department of Environment for making this research feasible.

References

ALabdeh, D., Omidvar, B., Karbassi, A., Sarang, A., 2020. Study of speciation and spatial variation of pollutants in Anzali Wetland (Iran) using linear regression, Kriging and multivariate analysis. Environ. Sci. Pollut. Res. 27(14), 16827–16840. https://doi.org/10.1007/s11356-020-08126-3.

Amaral-Zettler, L. A., Zettler, E. R., Mincer, T. J., Klaassen, M. A., Gallager, S. M., 2021. Biofouling impacts on polyethylene density and sinking in coastal waters: A macro/micro tipping point?. Water Res. 201. https://doi.org/10.1016/j.watres.2021.117289.

Amini, Z., Malekmohammadi, B., Jafari, H. R., 2021. Role of participatory management in water health quality of the Anzali International Wetland, Iran. Reg. Stud. Mar. Sci. 42. https://doi.org/10.1016/j.rsma.2021.101615.

Andrady, A. L., 2011. Microplastics in the marine environment. Mar. Pollut. Bull. 62(8), 1596–1605. https://doi.org/10.1016/j.marpolbul.2011.05.030.

Bellasi, A., Binda, G., Pozzi, A., Galafassi, S., Volta, P., Bettinetti, R., 2020. Microplastic contamination in freshwater environments: A review, focusing on interactions with sediments and benthic organisms. Environments – MDPI. 7(4). https://doi.org/10.3390/environments7040030.

Browne, M. A., Crump, P., Niven, S. J., Teuten, E., Tonkin, A., Galloway, T., Thompson, R., 2011. Accumulation of microplastic on shorelines woldwide: Sources and sinks. Environ. Sci. Technol. 45(21), 9175–9179. https://doi.org/10.1021/es201811s.

Chowdhury, M. J., Nasrin, S., Faruque, M. A. Al., 2017. Significance of Agro-Textiles and Future Prospects in Bangladesh. Eur. Sci. J. 13(21), 139. https://doi.org/10.19044/esj.2017.v13n21p139.

do Sul, J. A. I., Costa, M. F., 2014. The present and future of microplastic pollution in the marine environment. Environ. Pollut. 185, 352-364. https://doi.org/10.1016/j.envpol.2013.10.036.

Dissanayake, P. D., Kim, S., Sarkar, B., Oleszczuk, P., Sang, M.k., Haque, M. N., Ahn, J. H., Bank, M. S., Ok, Y. S., 2022. Effects of microplastics on the terrestrial environment: A critical review. Environ. Res. 209, 112734. https://doi.org/10.1016/j.envres.2022.112734.

Duan, Z., Zhao, S., Zhao, L., Duan, X., Xie, S., Zhang, H., Liu, Y., Peng, Y., Liu, C., Wang, L., 2020. Microplastics in Yellow River Delta wetland: Occurrence, characteristics, human influences, and marker. Environ. Pollut. 258. https://doi.org/10.1016/j.envpol.2019.113232.

Duan, J., Han, J., Cheung, S. G., Chong, R. K. Y., Lo, C. M., Lee, F. W. F., Xu, S. J. L., Yang, Y., Tam, N. F. yee, Zhou, H. C., 2021. How mangrove plants affect microplastic distribution in sediments of coastal wetlands: Case study in Shenzhen Bay, South China. Sci. Total Environ 767. https://doi.org/10.1016/j.scitotenv.2020.144695.

Edo, C., González-Pleiter, M., Tamayo-Belda, M., Ortega-Ojeda, F. E., Leganés, F., Fernández-Piñas, F., Rosal, R., 2020. Microplastics in sediments of artificially recharged lagoons: Case study in a Biosphere Reserve. Sci. Total Environ. 729. https://doi.org/10.1016/j.scitotenv.2020.138824.

Elvers, B. (Ed.)., 2016. Ullmann's Polymers and Plastics: Products and Processes, Wiley-VCH Verlag GmbH & Company KGaA.

Esmaeilzadeh, M., Karbassi, A., Moattar, F., 2016a. Assessment of metal pollution in the Anzali Wetland sediments using chemical partitioning method and pollution indices. Acta Oceanol. Sin. 35(10), 28–36. https://doi.org/10.1007/s13131-016-0920-z.

Esmaeilzadeh, M., Karbassi, A., Moattar, F., 2016b. Heavy metals in sediments and their bioaccumulation in Phragmites australis in the Anzali wetland of Iran. Chin. J. Oceanol. Limnol. 34(4), 810–820. https://doi.org/10.1007/s00343-016-5128-8.

Esmaeilzadeh, M., Mahmoudpuor, E., Haghighat, S., Esmaeilzadeh, S., Aliani, H., Yazdanfar, N., 2021. Contamination and ecological risk assessment of trace elements in sediments of the Anzali Wetland, Northern Iran. Water Sci. Technol. 84(9), 2578–2590. https://doi.org/10.2166/wst.2021.455.

Firdaus, M., Trihadiningrum, Y., Lestari, P., 2020. Microplastic pollution in the sediment of Jagir Estuary, Surabaya City, Indonesia. Mar. Pollut. Bull. 150. https://doi.org/10.1016/j.marpolbul.2019.110790.

Norén, F., 2007. Small plastic particles in coastal Swedish waters. KIMO Sweden. KIMO Sweden.

Geyer, R., Jambeck, J. R., Law, K. L., 2017. Production, use, and fate of all plastics ever made. Sci. Adv. 3(7), e1700782. https://doi.org/10.1126/sciadv.1700782.

Govender, J., Naidoo, T., Rajkaran, A., Cebekhulu, S., Bhugeloo, A., 2020. Towards characterising microplastic abundance, typology and retention in mangrove-dominated estuaries. Water 12(10), 2802. https://doi.org/10.3390/w12102802.

Hassanzadeh, M., Zarkami, R., Sadeghi, R., 2021. Uptake and accumulation of heavy metals by water body and Azolla filiculoides in the Anzali wetland. Appl. Water Sci. 11(6). https://doi.org/10.1007/s13201-021-01428-y.

He, B., Wijesiri, B., Ayoko, G. A., Egodawatta, P., Rintoul, L., Goonetilleke, A., 2020. Influential factors on microplastics occurrence in river sediments. Sci. Total Environ. 738, 139901. https://doi.org/10.1016/j.scitotenv.2020.139901.

Helcoski, R., Yonkos, L. T., Sanchez, A., Baldwin, A. H., 2020. Wetland soil microplastics are negatively related to vegetation cover and stem density. Environ. Pollut. 256. https://doi.org/10.1016/j.envpol.2019.113391.

Hidalgo-Ruz, V., Gutow, L., Thompson, R. C., Thiel, M., 2012. Microplastics in the marine environment: A review of the methods used for identification and quantification. Environ. Sci. Technol. 46(6), 3060–3075. https://doi.org/10.1021/es2031505.

Ibrahim, Y. S., Hamzah, S. R., Khalik, W. M. A. W. M., Ku Yusof, K. M. K., Anuar, S. T., 2021. Spatiotemporal microplastic occurrence study of Setiu Wetland, South China Sea. Sci. Total Environ. 788. https://doi.org/10.1016/j.scitotenv.2021.147809.

Jambeck, J. R., Geyer, R., Wilcox, C., Siegler, T. R., Perryman, M., Andrady, A., Narayan, R Law, K. L., 2015. Plastic waste inputs from land into the ocean. Science. 347(6223), 768-771. DOI: 10.1126/science.1260352.

Kershaw, P., Turra, A., Galgani, F., 2019. Guidelines for the monitoring and assessment of plastic litter in the ocean: GESAMP Joint Group of Experts on the Scientific Aspects of Marine Environmental Protection. In Rep. Stud. GESAMP: Vol. no 99. GESAMP reports and studies. http://www.gesamp.org/publications/guidelines-for-the-monitoring-and-assessment-of-plastic-litter-in-the-ocean.

Lambert, S., Sinclair, C., Boxall, A., 2014. Occurrence, degradation, and effect of polymer-based materials in the environment. Rev Environ Contam Toxicol. Volume 227, 1-53. https://doi.org/10.1007/978-3-319-01327-5_1.

Li, J., Zhang, H., Zhang, K., Yang, R., Li, R., Li, Y., 2018. Characterization, source, and retention of microplastic in sandy beaches and mangrove wetlands of the Qinzhou Bay, China. Mar. Pollut. Bull. 136, 401–406. https://doi.org/10.1016/j.marpolbul.2018.09.025.

Li, R., Yu, L., Chai, M., Wu, H., Zhu, X., 2020. The distribution, characteristics and ecological risks of microplastics in the mangroves of Southern China. Sci. Total Environ. 708. https://doi.org/10.1016/j.scitotenv.2019.135025.

Liang, T., Lei, Z., Fuad, M. T. I., Wang, Q., Sun, S., Fang, J. K. H., Liu, X., 2022. Distribution and potential sources of microplastics in sediments in remote lakes of Tibet, China. Sci. Total Environ. 806, 150526. https://doi.org/10.1016/j.scitotenv.2021.150526.

Lusher, A., 2015. Microplastics in the marine environment: Distribution, interactions and effects. Marine Anthropogenic Litter, 245–307. https://doi.org/10.1007/978-3-319-16510-3_10.

Lusher, A. L., McHugh, M., Thompson, R. C., 2013. Occurrence of microplastics in the gastrointestinal tract of pelagic and demersal fish from the English Channel. Mar. Pollut. Bull. 67(1–2), 94–99. https://doi.org/10.1016/j.marpolbul.2012.11.028.

Maghsodian, Z., Sanati, A. M., Ramavandi, B., Ghasemi, A., Sorial, G. A., 2021. Microplastics accumulation in sediments and Periophthalmus waltoni fish, mangrove forests in southern Iran. Chemosphere. 264. https://doi.org/10.1016/j.chemosphere.2020.128543.

Manbohi, A., Mehdinia, A., Rahnama, R., Dehbandi, R., Hamzehpour, A., 2021. Spatial distribution of microplastics in sandy beach and inshore-offshore sediments of the southern Caspian Sea. Mar. Pollut. Bull. 169, 112578. https://doi.org/10.1016/j.marpolbul.2021.112578.

Mehdinia, A., Dehbandi, R., Hamzehpour, A., Rahnama, R., 2020. Identification of microplastics in the sediments of southern coasts of the Caspian Sea, north of Iran. Environ. Pollut. 258. https://doi.org/10.1016/j.envpol.2019.113738.

Naderi, M., Saatsaz, M., 2020. Impact of climate change on the hydrology and water salinity in the Anzali Wetland, northern Iran. Hydrol. Sci. J 65(4), 552–570. https://doi.org/10.1080/02626667.2019.1704761.

Naji, A., Nuri, M., Amiri, P., Niyogi, S., 2019. Small microplastic particles (S-MPPs) in sediments of mangrove ecosystem on the northern coast of the Persian Gulf. Mar. Pollut. Bull. 146, 305–311. https://doi.org/10.1016/j.marpolbul.2019.06.033.

Nizzetto, L., Bussi, G., Futter, M. N., Butterfield, D., Whitehead, P. G., 2016. A theoretical assessment of microplastic transport in river catchments and their retention by soils and river sediments. Environ. Sci.: Process. Impacts. 18(8), 1050-1059. https://doi.org/10.1039/c6em00206d.

Nematollahi, M. J., Moore, F., Keshavarzi, B., Vogt, R. D., Nasrollahzadeh Saravi, H., Busquets, R., 2020. Microplastic particles in sediments and waters, south of Caspian Sea:

Frequency, distribution, characteristics, and chemical composition. Ecotoxicol. Environ. Saf. 206. https://doi.org/10.1016/j.ecoenv.2020.111137.

Nematollahi, M. Javad., Keshavarzi, B., Moore, F., Esmaeili, H. R., Nasrollahzadeh Saravi H., Sorooshian, A., 2021. Microplastic fibers in the gut of highly consumed fish species from the southern Caspian Sea. Mar. Pollut. Bull. 168 (2021): 112461. https://doi.org/10.1016/j.marpolbul.2021.112461.

Nematollahi, M. J., Keshavarzi, B., Mohit, F., Moore, F., Busquets, R., 2022. Microplastic occurrence in urban and industrial soils of Ahvaz metropolis: a city with a sustained record of air pollution. Sci. Total Environ. 819, 152051. https://doi.org/10.1016/j.scitotenv.2021.152051.

Nor, N. H. M., Obbard, J. P., 2014. Microplastics in Singapore's coastal mangrove ecosystems. Mar. Pollut. Bull. 79(1-2), 278-283. https://doi.org/10.1016/j.marpolbul.2013.11.025.

Qian, J., Tang, S., Wang, P., Lu, B., Li, K., Jin, W., He, X., 2021. From source to sink: Review and prospects of microplastics in wetland ecosystems. Sci. Total Environ. 758. https://doi.org/10.1016/j.scitotenv.2020.143633.

Rasta, M., Sattari, M., Taleshi, M. S., Namin, J. I., 2020. Identification and distribution of microplastics in the sediments and surface waters of Anzali Wetland in the Southwest Caspian Sea, Northern Iran. Mar. Pollut. Bull. 160. https://doi.org/10.1016/j.marpolbul.2020.111541.

Rasta, M., Sattari, M., Taleshi, M. S., Namin, J. I., 2021. Microplastics in different tissues of some commercially important fish species from Anzali Wetland in the Southwest Caspian Sea, Northern Iran. Mar. Pollut. Bull. 169, 112479. https://doi.org/10.1016/j.marpolbul.2021.112479.

Razeghi, N., Hamidian, A. H., Wu, C., Zhang, Y., Yang, M., 2021. Scientific studies on microplastics pollution in Iran: An in-depth review of the published articles. Mar. Pollut. Bull. 162. https://doi.org/10.1016/j.marpolbul.2020.111901.

Sarkar, D. J., Das Sarkar, S., Das, B. K., Sahoo, B. K., Das, A., Nag, S. K., Manna, R. K., Behera, B. K., Samanta, S., 2021. Occurrence, fate and removal of microplastics as heavy metal vector in natural wastewater treatment wetland system. Water Res. 192. https://doi.org/10.1016/j.watres.2021.116853.

Shariati, S., Pourbabaee, A. A., Alikhani, H. A., Rezaei, K. A., 2019. Assessment of phthalic acid esters pollution in Anzali wetland, north of Iran. Int J Environ Sci Technol. 16(11), 7025–7036. https://doi.org/10.1007/s13762-018-2110-3.

Soltani, N., Keshavarzi, B., Moore, F., Busquets, R., Nematollahi, M. J., Javid, R., Gobert, S., 2022. Effect of land use on microplastic pollution in a major boundary waterway: The Arvand River. Sci. Total Environ. 830, 154728. https://doi.org/10.1016/j.scitotenv.2022.154728.

Suhogusoff, A. V., Hirata, R., Ferrari, L. C. K., Robertson, W. D., Stimson, J., Forbes, D., Blowes, D. W., 2019. Field performance of two on-site wastewater treatment systems using reactive media layers for nutrient and pathogen removal. J. Water Process Eng. 32, 100905. https://doi.org/10.1016/j.jwpe.2019.100905.

Thompson, R. C., Olsen, Y., Mitchell, R. P., Davis, A., Rowland, S. J., John, A. W., McGonigle, D., Russell, A. E., 2004. Lost at sea: where is all the plastic?. Science, 304(5672), 838-838. https://doi.org/10.1126/science.1094559.

Townsend, K. R., Lu, H. C., Sharley, D. J., Pettigrove, V., 2019. Associations between microplastic pollution and land use in urban wetland sediments. Environ. Sci. Pollut. Res. 26(22), 22551–22561. https://doi.org/10.1007/s11356-019-04885-w.

Wang, Q., Huang, K., Li, Y., Zhang, Y., Yan, L., Xu, K., Huang, S., Junaid, M., Wang, J., 2021. Microplastics abundance, distribution, and composition in freshwater and sediments from the largest Xijin Wetland Park, Nanning, South China. Gondwana Res. https://doi.org/10.1016/j.gr.2021.07.009.

Wang, Z. M., Wagner, J., Ghosal, S., Bedi, G., Wall, S., 2017. SEM/EDS and optical microscopy analyses of microplastics in ocean trawl and fish guts. Sci. Total Environ. 603, 616-626. https://doi.org/10.1007/978-3-030-10618-8_7-1.

Wen, X., Xu, P., Zeng, G., Huang, D., Hu, L., Wan, J., Deng, R., Du, C., Yin, L., Zhang, J., Tan, S., Yin, Q., 2018. Microplastic pollution in surface sediments of urban water areas in Changsha, China: Abundance, composition, surface textures. Mar. Pollut. Bull. 136, 414–423. https://doi.org/10.1016/j.marpolbul.2018.09.043.

Woodward, R.T., Wui, Y.S., 2001. The economic value of wetland services: a meta-analysis. Ecol. Econ. 37 (2), 257–270. https://doi.org/10.1016/S0921-8009 (00)00276-7.

Yao, P., Zhou, B., Lu, Y. H., Yin, Y., Zong, Y. Q., Chen, M. Te, O'Donnell, Z., 2019. A review of microplastics in sediments: Spatial and temporal occurrences, biological effects, and analytic methods. Quat. Int. 519, 274–281. https://doi.org/10.1016/j.quaint.2019.03.028.

Yuan, W., Liu, X., Wang, W., Di, M., Wang, J., 2019. Microplastic abundance, distribution and composition in water, sediments, and wild fish from Poyang Lake, China. Ecotoxicol. Environ. Saf. 170, 180-187. https:// doi: 10.1016/j.ecoenv.2018.11.126.

Zhou, Q., Tu, C., Fu, C., Li, Y., Zhang, H., Xiong, K., Zhao, X., Li, L., Waniek, J. J., Luo, Y., 2020. Characteristics and distribution of microplastics in the coastal mangrove sediments of China. Sci. Total Environ. 703. https://doi.org/10.1016/j.scitotenv.2019.134807.

Zhou, Q., Zhang, H., Fu, C., Zhou, Y., Dai, Z., Li, Y., Luo, Y., 2018. The distribution and morphology of microplastics in coastal soils adjacent to the Bohai Sea and the Yellow Sea. Geoderma. 322, 201-208. https://doi.org/10.1016/j.geoderma.2018.02.015.

Ziajahromi, S., Drapper, D., Hornbuckle, A., Rintoul, L., Leusch, F. D. L., 2020. Microplastic pollution in a stormwater floating treatment wetland: Detection of tyre particles in sediment. Sci. Total Environ. 713. https://doi.org/10.1016/j.scitotenv.2019.136356.

.

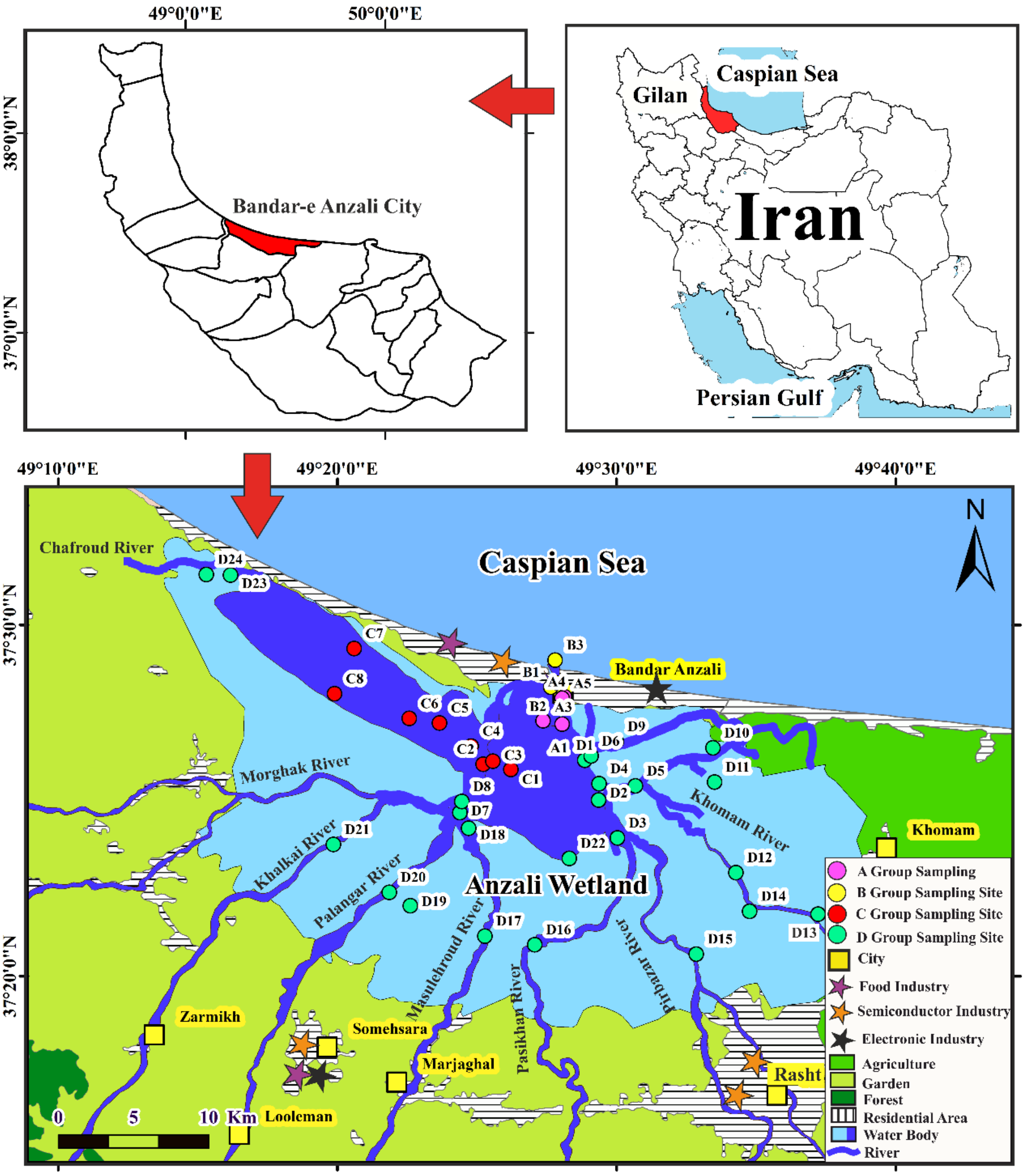

Fig. 1. Geographic position of the sediment sampling stations in the Anzali Wetland, Northern Iran.

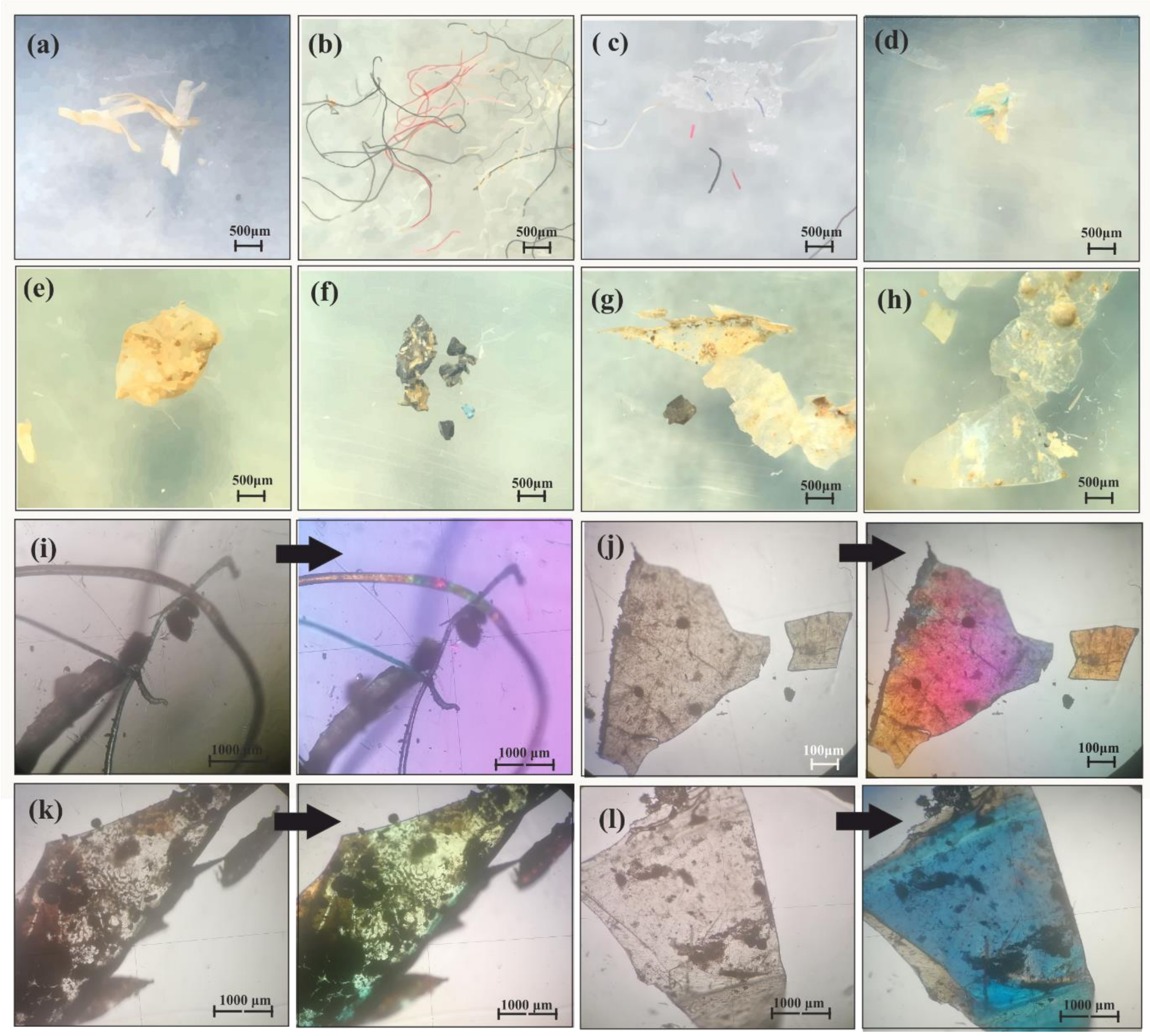

Fig. 2. Optical microscopy images of MP particles from wetland sediment samples. (a-c): fibers, (d-f): fragments, (g-h): films, and polarized light microscopy images: (i): fibers, (j-l): films.

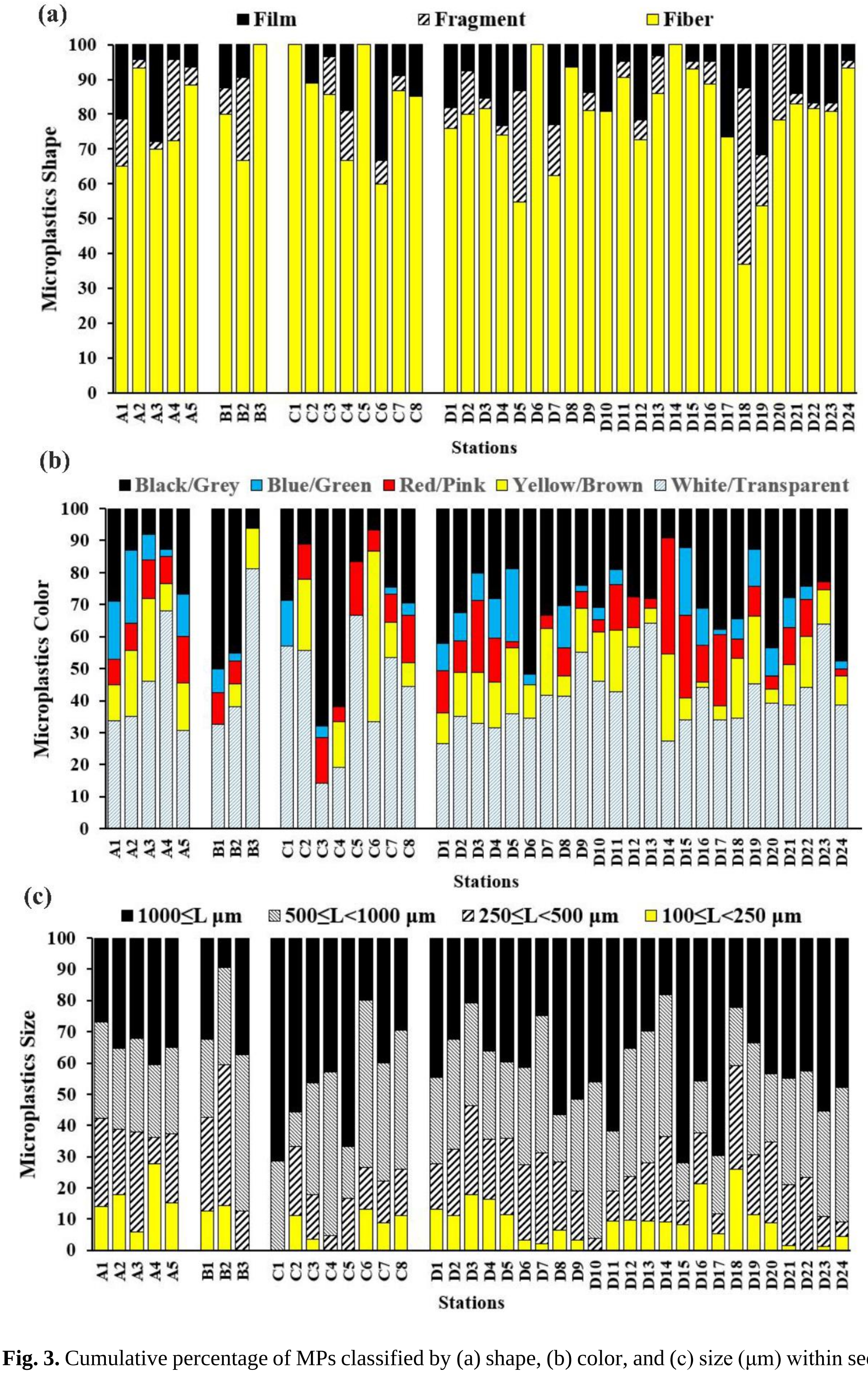

Fig. 3. Cumulative percentage of MPs classified by (a) shape, (b) color, and (c) size (μm) within sediment samples of Anzali Wetland.

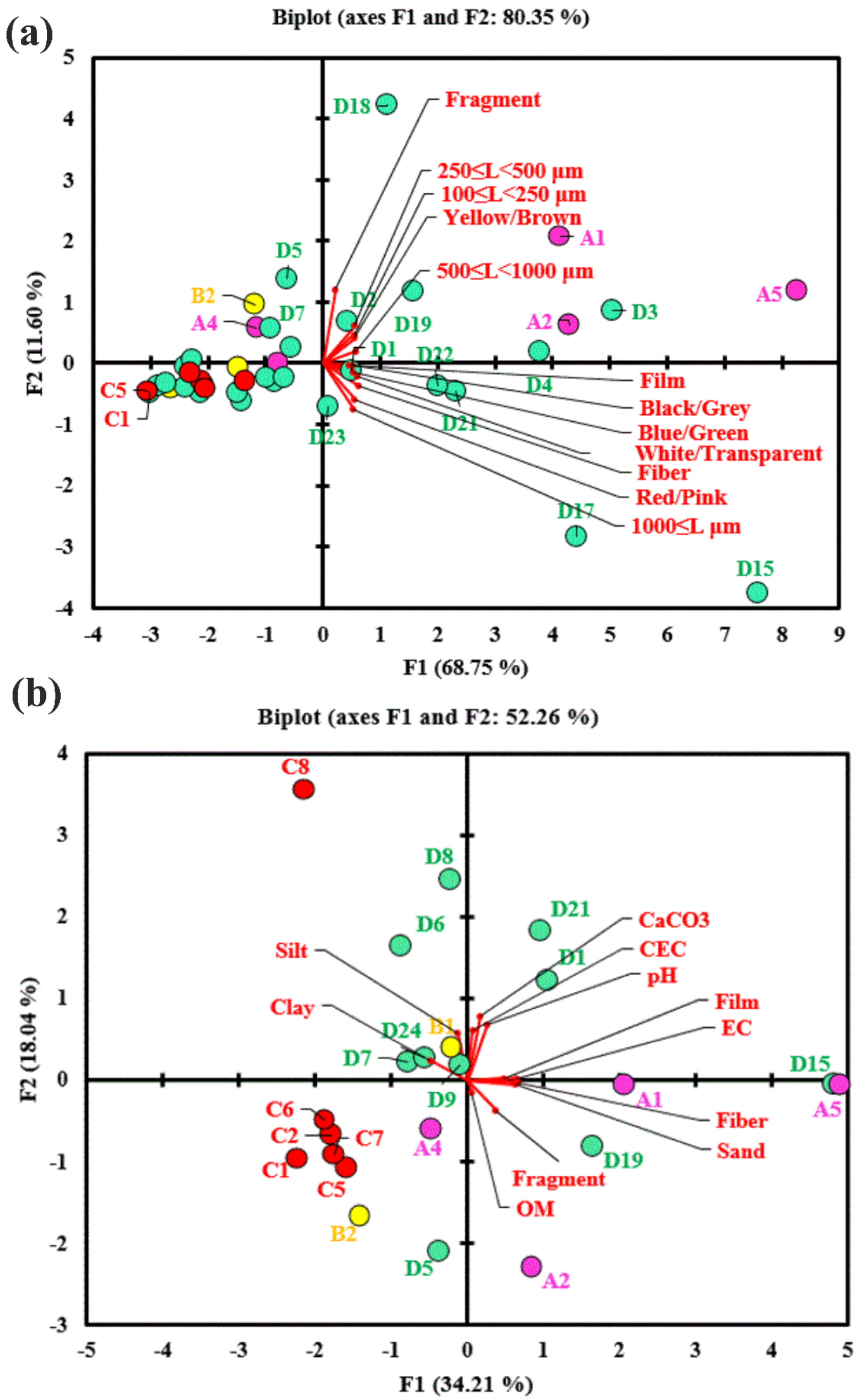

Fig. 4. PCA biplot for (a) MPs characteristics and (b) physico-chemical parameters of the sediment samples.

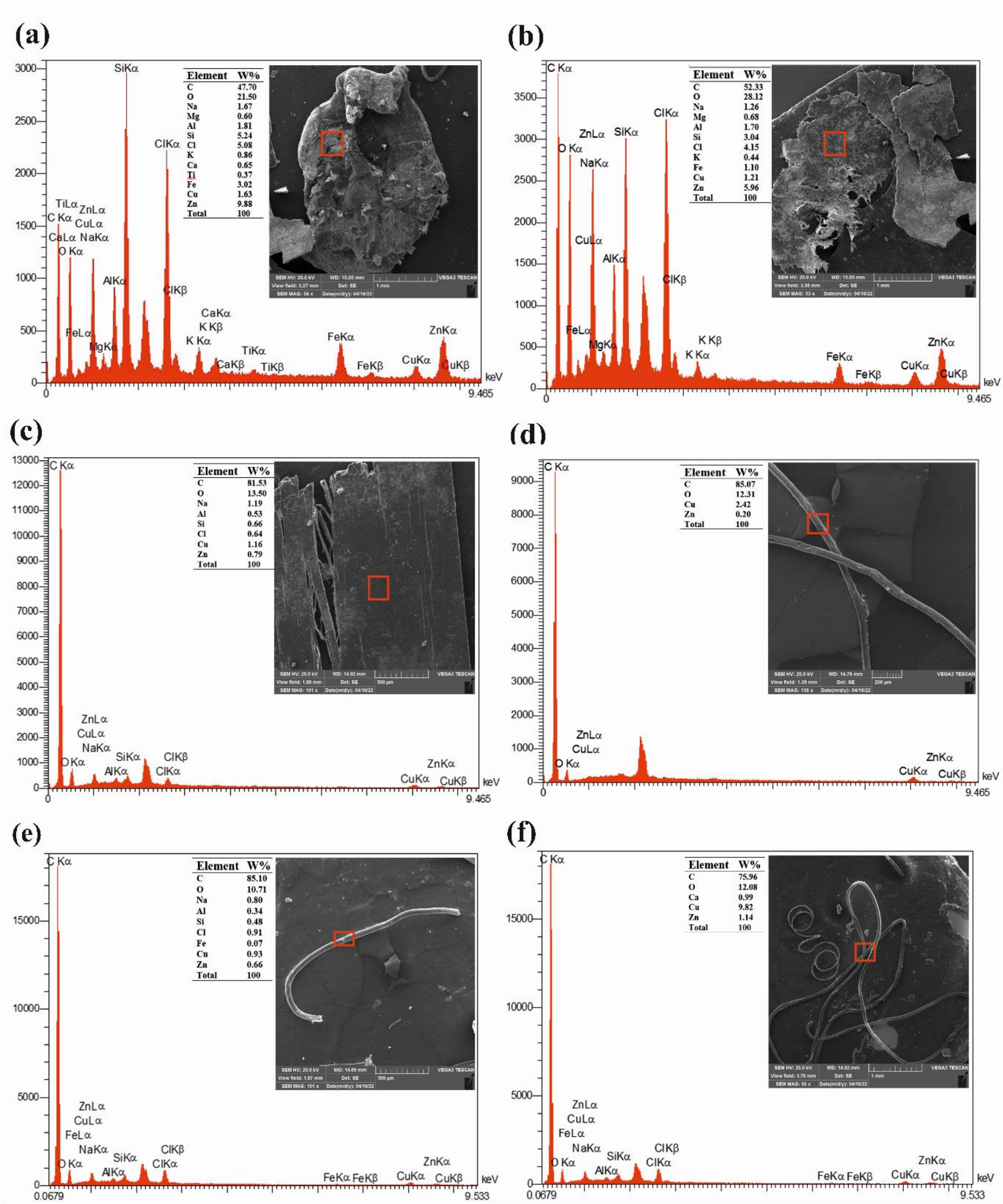

Fig. 5. SEM-EDS analyses of examined MPs in the sediments samples of Anzali Wetland (a) uneven surfaces with some attached particles on a weathered white polypropylene fragment, (b) a weathered and a non-weathered transparent low-density polyethylene film, (c) fracturing in a weathered white polypropylene film, (d) a weathered red polypropylene fiber, (e) a smooth transparent nylon fiber, and (f) two smooth black fibers with unknown polymeric composition.

Supporting Information S1. Further information on the study site

The Anzali Wetland supplies essential ecosystem services for residents and tourists, such as reducing contamination load of wastewater, stormwater management (flood control), biodiversity maintenance, water filtration, aesthetic values, and recreational values, as well as creating invaluable habitat for flora and fauna (Rasta et al., 2020). The highest elevation of the wetland basin is about 3105 m above sea level in the South, and the lowest is about 25 m under sea level in the north (Amini et al., 2021). The Anzali Wetland is the drainage basin of several seasonal and permanent rivers such as Chafroud, Morghak, Khalkai, Palangar, Masulehroud, Pasiphae, Pirbazar and Khomam streaming from Alborz and Talesh mountains (Fig. 1). The average water discharge into the wetland is about 76 m^3/s, and the total sediment load is about 683 K tones/year (Berenjkar et al., 2019). The wetland is surrounded by agricultural lands and protected scattered woodlands in the south (Naderi and Saatsaz, 2020). In addition to the Bandar-e Anzali city, which is situated close to the wetland, residential areas were scattered generally from the East where the capital city of the province, Rasht, is located, to the center of the catchment in adjacency to agricultural lands (Aghsaei et al., 2020) (Fig. 1). The wetland receives municipal wastewater effluents mainly through rivers and channels. The wetland discharges received contamination into the Caspian Sea via five canals in the northern parts (Hassanzadeh et al., 2021; Naderi and Saatsaz, 2020).

Supporting Information S2. Sample preparation

Sediments were sampled using a stainless Van Veen grab sampler and stainless-steel shovel from the top 15 cm of the sediment bed. Three sub-samples (totally 3 kg) were collected at each station in an area of approximately 1 m^2. The collected sub-samples were mixed and homogenized thoroughly to form a composite sample on pre-cleaned aluminum foil and transferred into aluminum foil bags. Samples were brought to the laboratory the same day for further processing. All bags were stored at -4 °C in the laboratory until further analysis. Each composite sample was divided into two subsamples. One part was dried at room temperature and sieved using a 2-mm metal sieve for physico-chemical parameters analysis. The other parts were transferred to glass beakers (pre-rinsed with distilled water) using a stainless steel spoon and dried at 50 °C for at least 48 h (Mehdinia et al., 2020). All dry samples were sieved using a 5 mm stainless steel mesh to separate larger particles. Sieved samples were transferred to 1 L beaker (pre-rinsed with distilled water) and were covered with aluminum foil.

Supporting Information S3. Extraction of MPs

The analytical method applied to extract MPs from the sediment samples was based on digesting organic matter followed by density separation of MPs as described elsewhere (Mehdinia et al., 2020; Nematollahi et al., 2020). In summary, each dry sediment sample (200 g) was transferred to a 1 L glass beaker (pre-rinsed with distilled water). In order to eliminate the interference of organic matters and improve the recognition of MPs, the sediment samples were mixed with 30% H_2O_2 for 7 days (Adomat and Grischek, 2020). Some filtered distilled water was added to the beaker to push adhered MPs on the wall of the glass beaker to the liquid. The beakers containing sediment samples in H_2O_2, covered with watch glasses, were placed onto the preheated sand bath at 50 °C until drying occurred (~2 days). The MPs were separated from the digested samples using buoyancy in 1.6 g cm^{-3} saturated $ZnCl_2$ salt solution (Loder and Gunner, 2015). The mixtures were covered with aluminum foil and they were left for 2 days to settle. After that, the supernatant was separated, centrifuged (5 min at 5000 rpm) and vacuum filtered through S&S filter paper (grade 589/3 blue ribbon, 2 µm pore size). The addition of $ZnCl_2$, centrifugation and filtration steps were carried out three times in total per digestate from 200g of sediment sample. The filters were left to dry inside closed cabinets and then transferred to Petri dishes (pre-cleaned with distilled water) for further steps. Sample blanks were carried out throughout the sample treatment and analysis of MPs.

Supporting Information S4. Physico-chemical parameters of the soil sediment samples

Half of the collected samples (n=22) were randomly selected for their characterization. This was because the sampling stations were in close proximity. Their particle size distribution was measured using the hydrometer method (Gee and Bauder, 1986). Their pH was determined in a homogeneous suspension of 10 g of sediment in 50 ml of distilled water, after 5 min shaking and 1 h pause. The pH of the unfiltered suspensions was specified using a combined glass electrode (Eutech instrument, Waterproof CyberScan PCD 650, Singapore) (Singh et al., 2005). A conductivity cell (CyberScan PCD 650) was used to measure electrical conductivity (EC) of the filtered suspension. The organic matters (OM) content in the sediment samples was assessed using loss on ignition method (Heiri et al., 2001). Cation exchange capacity (CEC) was estimated with the ammonium acetate solution method (Kahr and Madsen, 1995).

Supporting Information S5. Prevention of contamination

In sampling and analysis, we have tried to reduce MP contamination. Sampling equipment, containers and laboratory benches were thoroughly washed with filtered distilled water and immediately wrapped and covered with aluminum foil. Separation, counting and identification of MPs were conducted in a laboratory with closed doors and windows to mitigate MPs deposition from air. The experimental work included procedures that avoided contact with plastic materials. Cotton laboratory coats, and nitrile gloves were used during the sampling and laboratory processes (Adomat and Grischek, 2020). Beakers containing sieved samples were covered using aluminum foil (Irfan et al., 2020). The $ZnCl_2$ solution was filtered using S&S blue band filters (grade 589/3, 2 μm pore size) to ensure it was free from MPs. Filters were dried in closed cabinets wiped with tissue paper. Five uncovered and pre-cleaned glass Petri dishes were placed on the benches and exposed to the air during sample preparation and microscopy counting to assess airborne MPs contamination in the laboratory (Brander et al., 2020; Irfan et al., 2020; Wen et al., 2018). The laboratory blank tests indicated the possibility of MP particles contamination from the air was minor (totally 1 fiber was found) and could be neglected.

Supporting Information S6. Statistical analyses

Data analysis was done using Microsoft Excel 2016 and SPSS 26.0 software (IBMCo. Ltd., USA). The geographical distribution of sampling stations was shown using Arc Map (ver.10.6.1). Microplastic particles size was confirmed using microscopy and ImageJ software. Normality distribution of MPs abundance was checked using Kolmogorov–Smirnov test. Kruskal-Wallis (K-W) test was applied to examine significant differences ($p < 0.05$) between the abundance of MPs in different sampling regions. Principal component analysis (PCA) was performed using the XLSTAT 2016. The variables were normalized using the Kaiser method. Sample adequacy for PCA was checked using the Kaiser–Meyer–Olkin (KMO) method. Principal component analysis (PCA) using the eigenvalue decomposition (varimax rotation) method was applied to recognize relationships between MP properties, sediment physico-chemical parameters, and sampling sites.

Table S1 Comparison of abundance (MPs/kg), shape, sizes, color, and major types of MPs in this study with the some wetland sediments around the world.

Location	Abundance	Shape	Size	Color	Composition	Extraction/Identification Method	MPs Sources	Reference
Anzali Wetland	6-276 (72 ± 65.52[a]) (MPs/ 200g dw) 30-1380 (362.± 327.6[a])	Fiber (80.11%) Film (11.97%) Fragment (7.92%)	100≤L<250 µm (9.19%) 250≤L<500 µm (18.41%) 500≤L<1000 µm (31.43%) 1000 µm ≤L (40.97%)	White/Transparent (42.43%) Yellow/Brown/Orange (12.81%) Red/Pink/Purple (10.02%) Black/grey (28.20%)	PP (35%) PE (35%) NYL (13%) PC PET PVC	a) 30% H_2O_2 solution b) Density separation (using $ZnCl_2$ solution) c) Optical microscope d) Hot needle e) SEM-EDS f) Raman	A highly urbanized river	This study
Anzali Wetland	140–2820 (783.6 ± 877.8[a]) (June) 113–3690 (519.6 ± 1024.2[a]) (January)	Fiber (91.8% in June, 86.4% in January)	1–2 mm (36.7% in June and 34.8% in January)	Red (31.58%) Black (30.29%) Blue (23.34%)	PP (30.90 - 36.36) PEsT (21.21 – 25.45%) PAN PS PE	a) Density separation (using NaCl solution) b) Stereomicroscope c) Calibrated scaled eyepiece lens d) SEM-EDS e) ATR-FTIR	Untreated rivers, tourism activity, fishing and plastic bullet cases dropped from the guns of bird hunters	(Rasta et al., 2020)
Persian Gulf Iran	(19.5 ± 6.36[a] to 34.5 ± 0.71[a])	Fiber (>56%) Fragment (35%)	10-300 µm (70–97%)	Black (41%) Blue (18.4%) White (17.6%) Green (8.2%) Red (7%)	PE Nylon	a) Air-induced overflow b) NaCl and $ZnCl_2$ solution c) Stereomicroscope d) Hot needle e) SEM-EDS f) FTIR	Insufficiently treated and/or untreated effluent discharge from the surrounding cities	(Naji et al., 2019)
Greater Melbourne Australia	2-147 (46[b])	Fragment (>68%) Fiber Bead	<1000 µm	ND	ND	a) Density separation (using $ZnCl_2$ and NaCl solution) b) Microscope	Industrial activity, and plastic litter degradation	(Townsend et al., 2019)
Yellow River Delta China	136-2060	ND	ND	ND	PET PC	a) KOH and Pentanol solution at 135 °C b) Optical microscope	Human activities in the protection area	(Duan et al., 2020)
Kenilworth Park Washington, DC	334-3068 (1270 ± 150[a])	Fragment Fiber	75–5000 µm	ND	PS (29%) PE (8%) Rubber (8%)	a) 30% H_2O_2 solution and 0.05 M Fe(II) as $FeSO_4$ b) DI water c) Microscope d) FTIR	Highly urbanized river	(Helcoski et al., 2020)
Queensland's Gold Australia	(595 ± 12[a]) (inlet) (320 ± 42[a]) (outlet)	Fiber (>60%) Fragment Granular	>500 µm	ND	PP Nylon Acrylic Rubber	a) 30% H_2O_2 solution b) Density separation (using NaI solution) c) Staining with Rose-Bengal solution d) µ-ATR-FTIR	Transportation of synthetic rubber particles released from car tyres into wetland by road runoff and stormwater	(Ziajahromi et al., 2020)
Mangroves of Southern China	(227 ± 173[a] to 2249 ± 747[a])	Fiber Granule Film Foam	500–5000 µm (61.1%) 100-500 µm (19.8%) 50-100 µm (9.0%) < 50 µm (10.1%)	White/Transparent (80.60%) Black (10.52%) Blue (4.58%) Red (2.27%) Green (2.03%)	PP (67.47%) PE (13.05%) PS (10.45%)	a) H_2O_2 solution b) Density separation (using $ZnCl_2$ solution) c) µ-FTIR d) Stereomicroscope with electronic eyepiece e) SEM-EDS	Highly urbanized river	(Li et al., 2020)
Castilla-La Mancha Spain	(24.4 ± 5.2[a]) (particles/g dw) (24400 ± 5200[a])	Fiber (50-65%) Fragment (53%)	25–5000 µm	ND	PE and PP (90%)	a) 33% H_2O_2 solution b) Density separation (using NaCl solution) c) Stereomicroscope with Image Focus 4 camera d) ImageJ software e) µ-FTIR	Recharge of wetland with wastewater effluents to maintain water levels	(Edo et al., 2020)
Guangxi and Hainan China	8.3–5738.3	Foam (74.6%) Fiber (14.0%) Fragment	<2000 µm (58.6%)	White Transparent Green Blue Black	PS (75.2%) PP (11.7%) Rayon (4.6%) PES (3.4%) PE (2.8%) Acrylic (2.4%)	a) Density separation (using NaCl and NaI solution) b) Naked eye c) Stereomicroscope d) ATR-FTIR e) µ-FTIR f) SEM-EDS	Local agriculture and tourism/recreational activities	(Zhou et al., 2020)
Setiu Wetland South China Sea	(0.750 ± 3.838[a] to 14.25 ± 4.343[a]) (MPs/g dw) (750±3838[a] to 14250±4343[a])	Filament (98.49%) Fragment Film	ND	Transparent Brown Red Blue Green Black	PP	a) Density separation (using NaCl solution) b) Microscope c) Hot needle test d) Dyno-eye camera e) SEM f) ATR-DTGS-FTIR g) Pyr–GC/MS	Fisheries and aquaculture activities	(Ibrahim et al., 2021)
East Kolkata Eastern India	2125-6886.76	Film (80-95%) Fiber (5-20%)	63– 5000 µm	Transparent Multicolor	PE (37-50%) PET (31-45%)	a) 30% H_2O_2 solution b) Density separation (using $ZnCl_2$ solution) c) Microscope d) ATR-FTIR	Transport of microplastics through wastewater canals	(Sarkar et al., 2021)
Futian South China	2835 ± 713[a]	Fiber Granule Fragment Foam	ND	Black White Red Transparent	PET (43.83–57.22%) PP (25.06–32.86%) PS PA	a) 30% H_2O_2 solution b) Density separation (using $ZnCl_2$ solution) c) Stereomicroscope d) SEM-EDS f) FTIR	A highly urbanized river	(Duan et al., 2021)
Xijin Wetland Park South China	4-148 (MPs/500g dw) 8-296	Fiber	<500 µm	White-Blue	Rayon (14.55%) PEST (9.09%) PE (8.18%)	a) 30% H_2O_2 solution b) Density separation (using $ZnCl_2$ solution) c) Stereomicroscope d) FTIR	Agricultural waste, domestic sewage, sand mining boats, cage culture, and fishery activities	(Wang et al., 2021)

ND : Non-detected.
[a] Mean±SD.
[b] Mean.

Table S2 PCA biplot eigenvector values of MPs characteristics**.**

Variables	F1	F2
Fiber	**0.333**	-0.198
Fragment	0.116	**0.651**
Film	**0.246**	-0.021
White/Transparent	**0.326**	-0.120
Yellow/Brown/Orange	**0.303**	0.225
Red/Pink/Purple	**0.300**	-0.326
Blue/Green	**0.290**	-0.080
Black/Grey	**0.291**	-0.019
$100 \leq L < 250$ μm	**0.296**	0.256
$250 \leq L < 500$ μm	0.300	**0.335**
$500 \leq L < 1000$ μm	**0.316**	0.106
$1000 \leq L$ μm	**0.285**	-0.411

Table S3 Spearman correlation matrix of MPs characteristics.

Variables	Fiber	Fragment	Film	White/ Transparent	Yellow/ Brown	Red/ Pink	Blue/ Green	Black/ Grey	100≤L<250 µm	250≤L<500 µm	500≤L<1000 µm	1000≤L µm
Fiber	**1**											
Fragment	0.133	**1**										
Film	**0.559**	0.200	**1**									
White/Transparent	**0.934**	0.243	**0.662**	**1**								
Yellow/Brown	**0.782**	**0.361**	**0.565**	**0.769**	**1**							
Red/Pink	**0.913**	0.075	**0.580**	**0.824**	**0.605**	**1**						
Blue/Green	**0.868**	0.254	**0.348**	**0.759**	**0.736**	**0.777**	**1**					
Black/Grey	**0.775**	0.280	**0.745**	**0.746**	**0.597**	**0.701**	**0.512**	**1**				
100≤L<250 µm	**0.767**	**0.482**	**0.466**	**0.708**	**0.807**	**0.664**	**0.764**	**0.649**	**1**			
250≤L<500 µm	**0.743**	**0.474**	**0.573**	**0.730**	**0.889**	**0.578**	**0.667**	**0.710**	**0.837**	**1**		
500≤L<1000 µm	**0.831**	0.254	**0.708**	**0.858**	**0.876**	**0.653**	**0.632**	**0.800**	**0.734**	**0.883**	**1**	
1000≤L µm	**0.898**	0.061	**0.564**	**0.859**	**0.530**	**0.922**	**0.771**	**0.697**	**0.531**	**0.445**	**0.594**	**1**

Values in bold are different from 0 with a significance level alpha=0.05

Table S4 PCA biplot eigenvector values of soil sediment physico-chemical parameters**.**

	F1	F2
Sand	**0.526**	-0.053
Silt	0.219	0.348
Clay	-0.329	-0.127
pH	0.045	**0.634**
EC	**0.496**	-0.049
OM	-0.097	**0.638**
$CaCO_3$	-0.004	**0.122**
CEC	-0.127	**0.184**
MPs	**0.542**	-0.015

Table S5 Spearman correlation matrix of soil sediment physico-chemical parameters.

Variables	Sand	Silt	Clay	pH	EC	OM	$CaCO_3$	CEC	MPs
Sand	**1**								
Silt	0.174	**1**							
Clay	-0.354	-0.288	**1**						
pH	0.060	0.368	-0.057	**1**					
EC	**0.747**	0.259	-0.331	0.065	**1**				
OM	-0.187	0.256	-0.062	**0.906**	-0.196	**1**			
$CaCO_3$	-0.046	0.185	-0.061	0.034	-0.105	0.085	**1**		
CEC	-0.162	-0.133	-0.038	0.164	-0.226	0.219	-0.068	**1**	
MPs	**0.944**	0.236	-0.498	0.068	**0.752**	-0.170	0.008	-0.061	**1**

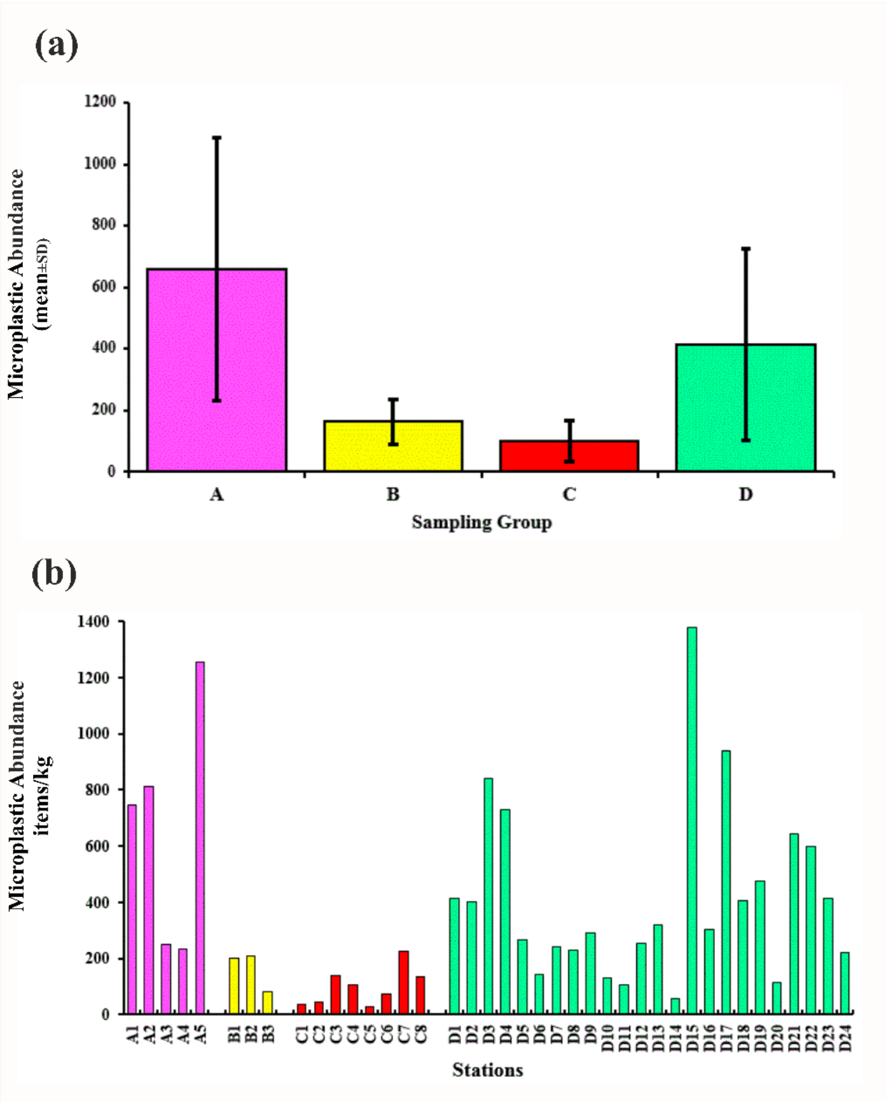

Fig. S1. Abundance of MPs (a) in different sampling groups and (b) sites**.**

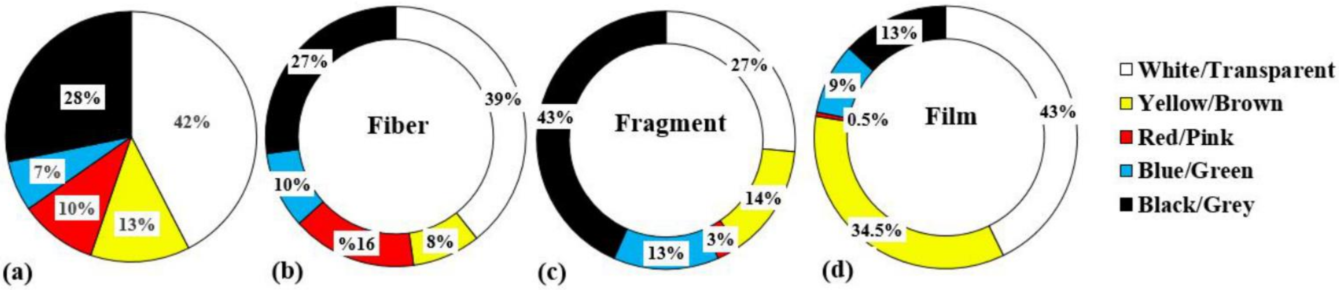

Fig. S2. Distribution of color classes of MPs in a) all detected MPs, b) Fibers, c) Fragments, and d) Films.

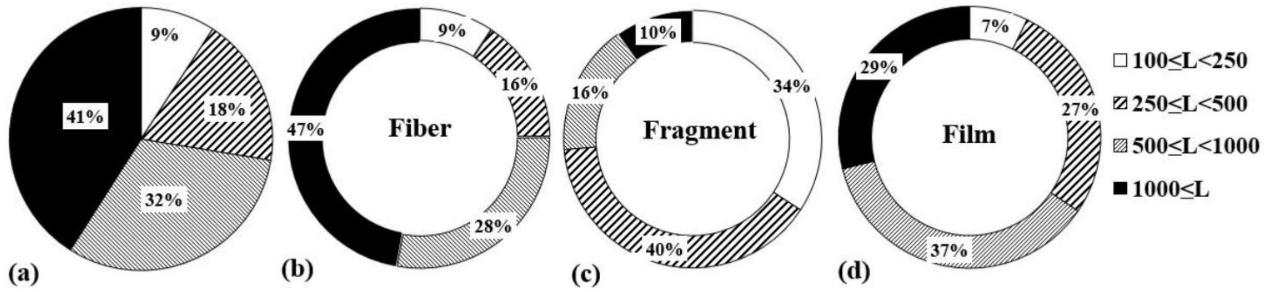

Fig. S3. Distribution of size classes (in μm) of MPs in a) all detected MPs, b) Fibers, c) Fragments, and d) Films.

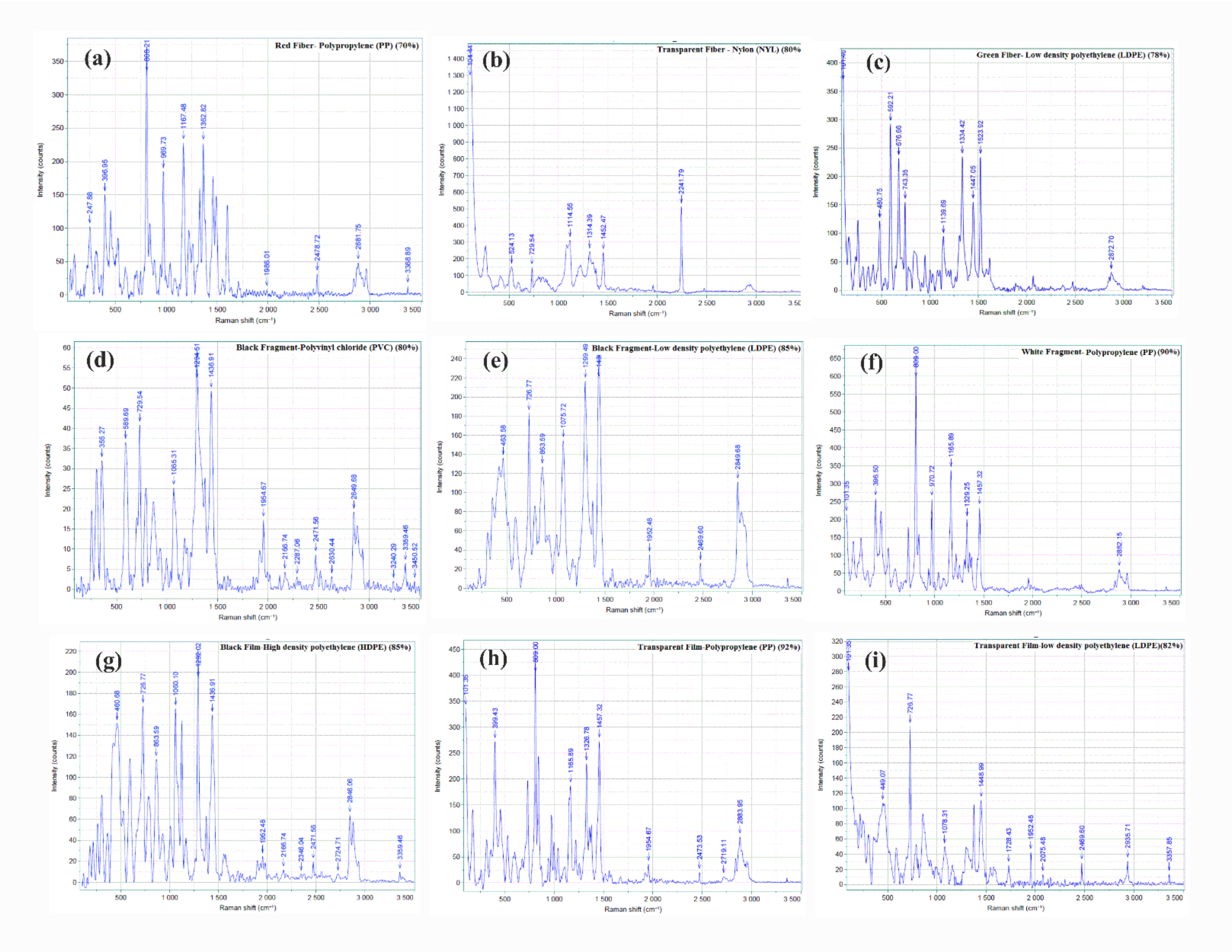

Fig. S4. Raman spectra of representative MPs identified in the study area, a) polypropylene (PP) red fiber with a mean match degree of 70%, b) nylon (NYL) transparent fiber with a mean match degree of 80%, c) low density polyethylene (LDPE) green fiber with a mean match degree of 78%, d) polyvinyl chloride (PVC) black fragment with a mean match degree of 80%, e) low density polyethylene (LDPE) black fragment with a mean match degree of 85%, f) polypropylene (PP) white fragment with a mean match degree of 90%, g) high density polyethylene (HDPE) black film with a mean match degree of 85%, h) polypropylene (PP) transparent film with a mean match degree of 92%, i) low density polyethylene (LDPE) transparent film with a mean match degree of 82%.

References

Adomat, Y., Grischek, T., 2020. Sampling and processing methods of microplastics in river sediments - A review. Sci. Total Environ. 758. https://doi.org/10.1016/j.scitotenv.2020.143691.

Aghsaei, H., Mobarghaee Dinan, N., Moridi, A., Asadolahi, Z., Delavar, M., Fohrer, N., Wagner, P. D., 2020. Effects of dynamic land use/land cover change on water resources and sediment yield in the Anzali wetland catchment, Gilan, Iran. Sci. Total Environ. 712. https://doi.org/10.1016/j.scitotenv.2019.136449.

Amini, Z., Malekmohammadi, B., Jafari, H. R., 2021. Role of participatory management in water health quality of the Anzali International Wetland, Iran. Reg. Stud. Mar. Sci. 42. https://doi.org/10.1016/j.rsma.2021.101615.

Berenjkar, P., Saeedi, M., Yuan, Q., 2019. Assessment of heavy metal release from dredged materials for different disposal scenarios: Study of Anzali international wetland, Iran. Process Saf. Environ. Prot. 132, 94–104. https://doi.org/10.1016/j.psep.2019.10.008.

Brander, S. M., Renick, V. C., Foley, M. M., Steele, C., Woo, M., Lusher, A., Carr, S., Helm, P., Box, C., Cherniak, S., Andrews, R. C., Rochman, C. M., 2020. Sampling and Quality Assurance and Quality Control: A Guide for Scientists Investigating the Occurrence of Microplastics across Matrices. Appl. Spectrosc. 74 (9), 1099–1125. https://doi.org/10.1177/0003702820945713.

Duan, J., Han, J., Cheung, S. G., Chong, R. K. Y., Lo, C. M., Lee, F. W. F., Xu, S. J. L., Yang, Y., Tam, N. F. yee, Zhou, H. C., 2021. How mangrove plants affect microplastic distribution in sediments of coastal wetlands: Case study in Shenzhen Bay, South China. Sci. Total Environ. 767. https://doi.org/10.1016/j.scitotenv.2020.144695.

Duan, Z., Zhao, S., Zhao, L., Duan, X., Xie, S., Zhang, H., Liu, Y., Peng, Y., Liu, C., Wang, L., 2020. Microplastics in Yellow River Delta wetland: Occurrence, characteristics, human influences, and marker. Environ. Pollut. 258. https://doi.org/10.1016/j.envpol.2019.113232.

Edo, C., González-Pleiter, M., Tamayo-Belda, M., Ortega-Ojeda, F. E., Leganés, F., Fernández-Piñas, F., Rosal, R., 2020. Microplastics in sediments of artificially recharged lagoons: Case study in a Biosphere Reserve. Sci. Total Environ. 729. https://doi.org/10.1016/j.scitotenv.2020.138824.

Gee, G., Bauder, J., 1986. Particle-size analysis. In: Klute, A. (Ed.), Methods of Soil Analysis. Part 1. Physical and Mineralogical Methods. Soil Sci. Soc. Am. Madison, WI, pp. 383–411.

Hassanzadeh, M., Zarkami, R., Sadeghi, R., 2021. Uptake and accumulation of heavy metals by water body and Azolla filiculoides in the Anzali wetland. Appl. Water Sci. 11(6). https://doi.org/10.1007/s13201-021-01428-y.

Heiri, O., Lotter, A. F., Lemcke, G., 2001. Loss on ignition as a method for estimating organic and carbonate content in sediments: reproducibility and comparability of results. J Paleolimnol. 25 (1): 101–110. https://doi.org/10.1023/A:1008119611481.

Helcoski, R., Yonkos, L. T., Sanchez, A., Baldwin, A. H., 2020. Wetland soil microplastics are negatively related to vegetation cover and stem density. Environ. Pollut. 256. https://doi.org/10.1016/j.envpol.2019.113391.

Ibrahim, Y. S., Hamzah, S. R., Khalik, W. M. A. W. M., Ku Yusof, K. M. K., Anuar, S. T., 2021. Spatiotemporal microplastic occurrence study of Setiu Wetland, South China Sea. Sci. Total Environ. 788. https://doi.org/10.1016/j.scitotenv.2021.147809.

Irfan, T., Khalid, S., Taneez, M., Hashmi, M. Z., 2020. Plastic driven pollution in Pakistan: the first evidence of environmental exposure to microplastic in sediments and water of Rawal Lake. Environ. Sci. Pollut. Res. 27(13), 15083–15092. https://doi.org/10.1007/s11356-020-07833-1.

Kahr, G., Madsen, F. T., 1995. Determination of the cation exchange capacity and the surface area of bentonite, illite and kaolinite by methylene blue adsorption. Appl. Clay Sci. 9(5), 327-336. https://doi.org/10.1016/0169-1317(94)00028-O.

Li, R., Yu, L., Chai, M., Wu, H., Zhu, X., 2020. The distribution, characteristics and ecological risks of microplastics in the mangroves of Southern China. Sci. Total Environ. 708. https://doi.org/10.1016/j.scitotenv.2019.135025.

Loder, M., Gunner, G., 2015. Methodology Used for the Detection and Identification of Microplastics—A Critical Appraisal. Marine Anthropogenic Litter, 201–227. https://doi.org/10.1007/978-3-319-16510-3_8.

Mehdinia, A., Dehbandi, R., Hamzehpour, A., Rahnama, R., 2020. Identification of microplastics in the sediments of southern coasts of the Caspian Sea, north of Iran. Environ. Pollut. 258. https://doi.org/10.1016/j.envpol.2019.113738.

Naderi, M., Saatsaz, M., 2020. Impact of climate change on the hydrology and water salinity in the Anzali Wetland, northern Iran. Hydrol. Sci. J. 65(4), 552–570. https://doi.org/10.1080/02626667.2019.1704761.

Naji, A., Nuri, M., Amiri, P., Niyogi, S., 2019. Small microplastic particles (S-MPPs) in sediments of mangrove ecosystem on the northern coast of the Persian Gulf. Mar. Pollut. Bull. 146, 305–311. https://doi.org/10.1016/j.marpolbul.2019.06.033.

Nematollahi, M. J., Moore, F., Keshavarzi, B., Vogt, R. D., Nasrollahzadeh Saravi, H., Busquets, R., 2020. Microplastic particles in sediments and waters, south of Caspian Sea: Frequency, distribution, characteristics, and chemical composition. Ecotoxicol. Environ. Saf. 206. https://doi.org/10.1016/j.ecoenv.2020.111137.

Rasta, M., Sattari, M., Taleshi, M. S., Namin, J. I., 2020. Identification and distribution of microplastics in the sediments and surface waters of Anzali Wetland in the Southwest Caspian Sea, Northern Iran. Mar. Pollut. Bull. 160.

https://doi.org/10.1016/j.marpolbul.2020.111541.
Sarkar, D. J., Das Sarkar, S., Das, B. K., Sahoo, B. K., Das, A., Nag, S. K., Manna, R. K., Behera, B. K., Samanta, S., 2021. Occurrence, fate and removal of microplastics as heavy metal vector in natural wastewater treatment wetland system. Water Res. 192. https://doi.org/10.1016/j.watres.2021.116853.
Singh, K. P., Mohan, D., Singh, V. K., Malik, A., 2005. Studies on distribution and fractionation of heavy metals in Gomti river sediments—a tributary of the Ganges, India. J. Hydrol. 12(1-4), 14-27. https://doi.org/10.1016/j.jhydrol.2005.01.021.
Townsend, K. R., Lu, H. C., Sharley, D. J., Pettigrove, V., 2019. Associations between microplastic pollution and land use in urban wetland sediments. Environ. Sci. Pollut. Res. 26(22), 22551–22561. https://doi.org/10.1007/s11356-019-04885-w.
Wang, Q., Huang, K., Li, Y., Zhang, Y., Yan, L., Xu, K., Huang, S., Junaid, M., Wang, J., 2021. Microplastics abundance, distribution, and composition in freshwater and sediments from the largest Xijin Wetland Park, Nanning, South China. Gondwana Res. https://doi.org/10.1016/j.gr.2021.07.009.
Wen, X., Xu, P., Zeng, G., Huang, D., Hu, L., Wan, J., Deng, R., Du, C., Yin, L., Zhang, J., Tan, S., Yin, Q., 2018. Microplastic pollution in surface sediments of urban water areas in Changsha, China: Abundance, composition, surface textures. Mar. Pollut. Bull. 136, 414–423.
Zhou, Q., Tu, C., Fu, C., Li, Y., Zhang, H., Xiong, K., Zhao, X., Li, L., Waniek, J. J., Luo, Y., 2020. Characteristics and distribution of microplastics in the coastal mangrove sediments of China. Sci. Total Environ. 703. https://doi.org/10.1016/j.scitotenv.2019.134807.
Ziajahromi, S., Drapper, D., Hornbuckle, A., Rintoul, L., Leusch, F. D. L., 2020. Microplastic pollution in a stormwater floating treatment wetland: Detection of tyre particles in sediment. Sci. Total Environ. 713. https://doi.org/10.1016/j.scitotenv.2019.136356